


Research Article

Heterologous Prime-boost with Chimpanzee Adenovirus Vector and Receptor-Binding Domain Recombinant Subunit Protein COVID-19 Vaccine Induces Strong Immune Responses in Mice

Qinhua Peng^{1,4}, Xiaohong Wu^{1,4}, Xingxing Li^{1,4}, Zelun Zhang^{1,2,4}, Hongshan Xu^{1,4}, Xinyu Liu¹, Wenjuan Li¹, Miao Li^{1,3}, Enyue Fang^{1,4}, Xiaohui Liu^{1,3}, Jingjing Liu¹, Danhua Zhao¹, Lihong Yang¹, Hongyu Wang¹, Jia Li¹, Yanqiu Huang¹, Leitai Shi¹, Yunpeng Wang¹, Ren Yang¹, Guangzhi Yue¹, Yue Suo¹, Min Li^{2,5}, Shouchun Cao^{1,2}, Qiang Ye^{1,2}, and Yuhua Li^{1,*}

Abstract

Several vaccines for coronavirus disease 2019 have been developed worldwide. A heterologous prime-boost strategy has been identified as a potential method for achieving potent immunity against severe acute respiratory syndrome coronavirus 2 (SARS-CoV-2). Herein, by adopting pathogen-free, female BALB/c mice, the present work assessed diverse prime-boosted strategies using the chimpanzee adenovirus vector-based vaccine, ChAdTS-S (ChAd), together with the recombinant subunit vaccine, ZF2001. Animals were divided into 12 groups (n = 5 per group) for immunization according to the corresponding immunization procedures. ChAd was given through intranasal (i.n.) or intramuscular i.m. administration, while ZF2001 through i.m. administration. At 42 days after primary immunization, the highest specific pseudovirus-neutralizing antibody (PNAb) and IgG levels against the Wuhan-Hu-1 strain were induced in the heterologous prime-boost group i.m. ChAd > i.m. ZF2001 group) among all the different vaccination combination groups. In addition, the i.n.-administered ChAd group induced higher PNAb to resist the Wuhan-Hu-1 strain in comparison with the i.m.-administered ChAd group. All vaccination groups exhibited low vaccine-induced PNAb levels to resist the B.1.1.529 strain. Higher IgA levels were induced in the i.n. vaccination-containing groups. The i.m. ZF2001 > i.n. ChAd strategy exhibited the highest angiotensin-converting enzyme-2-binding inhibition level for resisting diverse SARS-CoV-2 variants. All vaccinations triggered Th1-biased cellular immunity. Among these, the i.m.-administered ChAd strategy induced higher levels of Th1 cytokines compared to those induced with i.n.-administered ChAd. This study provides reference data for optimizing the heterologous prime-boost vaccination strategy against COVID-19.

Keywords: SARS-CoV-2, AdC68-19S, ChAdOx1 nCoV-19, NVX-CoV2373, NIFDC

Introduction

The COVID-19 pandemic has prevailed for over two years. The immune escape phenomenon of a variety of existing variants of concern (VOC) of the severe acute respiratory syndrome coronavirus 2 (SARS-CoV-2) (Alpha [B.1.1.7], Beta [B.1.351], Gamma [P.1], Delta [B.1.617.2], and Omicron [B.1.1.529]) is a predominant contributing factor to the continued epidemic

Affiliation:

¹Department of Arboviral Vaccine, National Institutes for Food and Drug Control, Beijing, China
²Division of in vitro Diagnostic Reagents, National Institutes for Food and Drug Control, Beijing, China
³Vaccines R&D Department, Changchun Institute of Biological Products Co. Ltd., Changchun, China
⁴Institute of Health Quarantine, Chinese Academy of Laboratory of Regulatory Science, Beijing, China
⁵Center for drug evaluation. NMPA; office of pharmaceutical science of biological products, Beijing, China

*Corresponding author:

Min Li, Center for drug evaluation. NMPA; office of pharmaceutical science of biological products, Beijing, China.
 Shouchun Cao, Department of Arboviral Vaccine, National Institutes for Food and Drug Control, Beijing, China.
 Qiang Ye, Department of Arboviral Vaccine, National Institutes for Food and Drug Control, Beijing, China.
 Yuhua Li, Department of Arboviral Vaccine, National Institutes for Food and Drug Control, Beijing, China.

Citation: Qinhua Peng, Xiaohong Wu, Xingxing Li, Zelun Zhang, Hongshan Xu, Xinyu Liu, Wenjuan Li, Miao Li, Enyue Fang, Xiaohui Liu, Jingjing Liu, Danhua Zhao, Lihong Yang, Hongyu Wang, Jia Li, Yanqiu Huang, Leitai Shi, Yunpeng Wang, Ren Yang, Guangzhi Yue, Yue Suo, Min Li, Shouchun Cao, Qiang Ye and Yuhua Li. Heterologous Prime-boost with Chimpanzee Adenovirus Vector and Receptor-Binding Domain Recombinant Subunit Protein COVID-19 Vaccine Induces Strong Immune Responses in Mice. *Archives of Microbiology and Immunology*. 7 (2023): 408-420.

Received: November 15, 2023

Accepted: November 22, 2023

Published: December 13, 2023

of COVID-19 [1–6]. Based on statistics provided by the World Health Organization [6], approximately 590 million of the global population are affected by SARS-CoV-2, with 6.46 million of them dying of this disease. Up to 23 August 2022, approximately 12.4 billion COVID-19 vaccine doses were administered around the world [6]. Many vaccines have been designed against the Wuhan-Hu-1 strain, but various data have shown that vaccine protection efficiency for other SARS-CoV-2 variants has decreased to varying degrees [7–9]. For example, Vimvara et al. [10] tested neutralizing antibodies against different strains in the serum of medical staff inoculated with two doses of CoronaVac, and the results showed that the neutralizing antibodies produced against other variants decreased remarkably compared with Wuhan-Hu-1. In addition, the existing COVID-19 vaccines, using homologous prime-boost strategies, cannot achieve adequate protection against new SARS-CoV-2 variants. Therefore, exploring more effective SARS-CoV-2 immunization strategies and vaccination routes is urgently required. Adenovirus vectors have the advantages of easy genetic manipulation, high immunogenicity, short production cycles, and demonstrable safety [11]. Adenoviruses from chimpanzees are widely used because of their low pre-existing immunity [12]. The serum prevalence of chimpanzee adenovirus type 68 in the Chinese population is only approximately 12.7%. However, the serum prevalence of human adenovirus type 5 in the Chinese population is as high as 73.1% [13]. Furthermore, multiple studies have shown that vaccines based on chimpanzee adenovirus type 68 show high immunogenicity in mice [14–16]. For example, as found by Li et al. [15], one individual intramuscular i.m. dose of an AdC68-19S vaccine induced a long-term and high systemic immune response to resist SARS-CoV-2 within BALB/c mice, which lasted for at least 40 weeks. Furthermore, one individual i.m. AdC68-19S dose demonstrated a high protective effect against SARS-CoV-2 within golden Syrian hamsters, which was demonstrated by challenge in week six after vaccination. Similar results were observed in non-human primate monkeys after the challenge in week eight. A two-dose SARS-CoV-2 vaccine based on the AstraZeneca chimpanzee adenovirus vector, ChAdOx1 nCoV-19, showed great safety as well as immunogenicity against Wuhan-Hu-1 in phase 1–3 clinical trials [17,18]. However, protection from variants induced by ChAdOx1 nCoV-19 significantly decreased, with a 1.3–31.5-fold reduction in efficacy compared to its effects against Wuhan-Hu-1 [7,19]. Multiple data [20–22] show higher neutralizing antibodies and protection efficiency induced by adenovirus vector-based vaccines administered via the intranasal (i.n.) route than by the i.m. route. Adenovirus vector-based vaccines delivered via the mucosal route may be beneficial in dealing with immune escape by multiple emerging variants.

Currently, recombinant subunit SARS-CoV-2 vaccines, including NVX-CoV2373 (Novavax) and ZF2001 (Chongqing Zhifei Biological Products Co., Ltd.), show approximately 90% protection against the Wuhan-Hu-1 strain [23,24]; however, they have shown significantly lower protective efficiency against the new SARS-CoV-2 variants, especially the Omicron strains [25–27]. Low cellular immune responses have been a disadvantage for recombinant subunit vaccines [28]. However, Tarke et al. [29] showed that T cell immune responses have more conserved epitope peptide regions compared to B cell immune responses, thereby inducing higher cross-protection against emerging variants. Therefore, improving the cellular immune response of recombinant subunit vaccines may break the immune bottleneck of vaccines to resist new SARS-CoV-2 variants. The heterologous prime-boost strategy can overcome immunity and fundamentally improve the systemic immune response relative to the homologous prime-boost strategy [30–32]. Consequently, the present work focused on exploring the immunogenicity of heterologous prime-boost strategies by adopting a vaccine based on chimpanzee adenovirus vector, ChAdTS-S (ChAd), along with a recombinant subunit vaccine, ZF2001, using pathogen-free, female BALB/c mice and different immunization routes. The aim was to fundamentally break the immune bottleneck of the two COVID-19 vaccines and provide a database for the optimization of immunization strategies and the improvement of COVID-19 vaccine-induced cross-protection.

Materials and Methods

Animals and vaccines

Animal experiments are conducted in strict accordance with the Guidelines for the Care and Use of Laboratory Animals of the People's Republic of China. This study has been approved by the Animal Care & Welfare Committee of National Institutes for Food and Drug Control (NIFDC). The mice were not anesthetized during the experiment, and at the end of all experiments, all mice were sacrificed by CO₂ euthanasia. All procedures involving animal testing are designed to avoid or minimize animal discomfort. The mice were maintained under SPF conditions and allowed free access to water and food. All vaccines utilized in the present work were ChAdTS-S (ChAd, 1 × 10¹¹ VP/0.5 mL, Walvax Biotechnology Co., Ltd.) and the recombinant subunit vaccine, ZF2001 (50 µg/1.0 mL [2 doses], Anhui Zhifei Longcom Biopharmaceutical Co., Ltd.). Animals were divided into 12 groups (n = 5 per group) for immunization according to diverse immunization procedures, as follows:

A. Heterologous prime-boost groups (groups 1–4):

1. i.n. ChAd > i.m. ZF2001
2. i.m. ZF2001 > i.n. ChAd

- 3. i.m. ChAd > i.m. ZF2001
- 4. i.m. ZF2001 > i.n. ChAd
- B. Mixed vaccination group (group 5):
- 5. i.m. ZF2001+ChAd
- C. ChAd control groups (groups 6–9):
- 6. × i.n. ChAd
- 7. × i.m. ChAd
- 8. × i.n. ChAd
- 9. × i.m. ChAd
- D. ZF2001 control group (group 10):
- 10. 2 × i.m. ZF2001
- E. Blank control groups (groups 11–12):
- 11. i.n. blank
- 12. i.m. blank

Group numbers, group names, and immunization strategies are shown in Fig. 1A. All vaccination strategies were administered on day 0 for the initial vaccination, and on day 28 for the booster vaccination. The dose of ChAd was 4×10^{10} VP per mouse, and the dose of ZF2001 was 10 µg per mouse. Sera were harvested from the mice at 14 and 42 days following primary immunization. The mice were sacrificed via cervical dislocation on day 56 for splenic lymphocyte isolation.

S protein-specific IgG and IgA titer measured by enzyme-linked immunosorbent assay (ELISA)

ELISA was conducted to analyze SARS-CoV-2 spike-specific IgG and IgA titers. In brief, we added 0.2 µg of the SARS-CoV-2 spike protein (Sino Biological, Beijing, China) to coat Corning ELISA plates (Corning, Inc., Corning, NY, USA) overnight. After washing with phosphate-buffered saline (PBS) containing 0.05% Tween 20 (PBST), the plates were subjected to 1-h blocking using PBST that contained 1% bovine serum albumin at 37°C. The plates were later rinsed by PBST six times, and four-fold serially

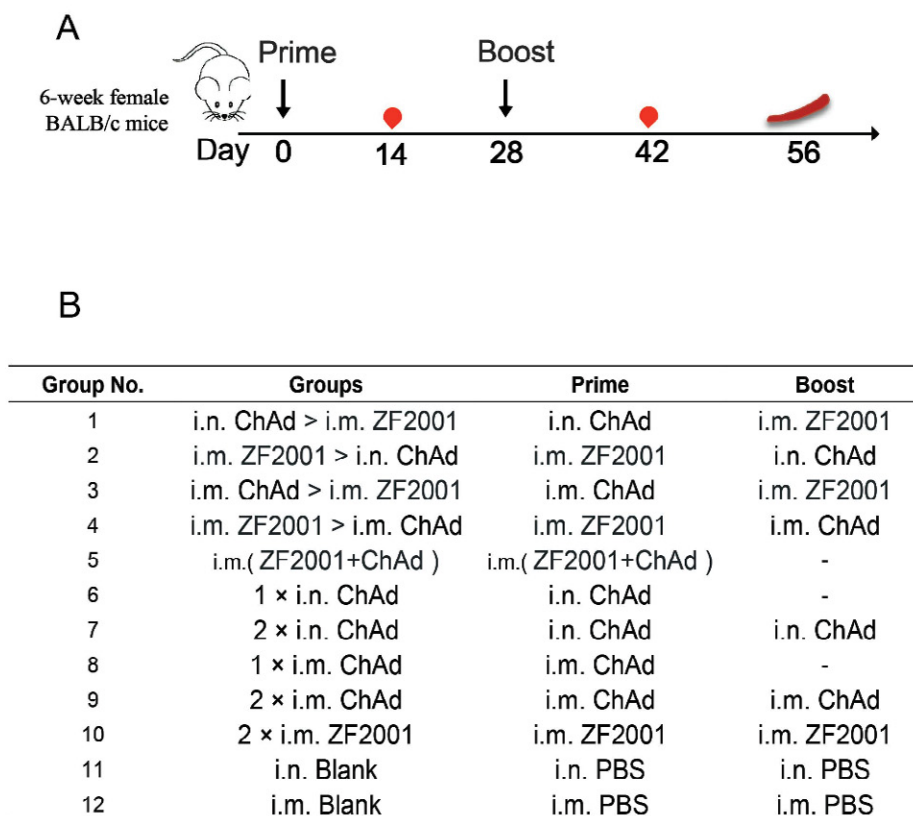


Figure 1: Female BALB/c immune grouping design, immunization strategies, and experimental timeline. (A) Immunization and immunological characterization scheme. Days 0 and 28, vaccination; days 14 and 42, blood sampling; day 56, sacrifice of the animal and spleen lymphocyte isolation. (B) Mice in the 12 groups were subjected to immunization using two COVID-19 vaccines in line with diverse instructions. The dash suggests the absence of a booster vaccination. ZF2001 represents the COVID-19 receptor-binding domain (RBD) dimer-based recombinant subunit vaccine. ChAd is a recombinant chimpanzee adenovirus vaccine ChAdTS-S. Abbreviations: i.m., vaccination administered intramuscularly; i.n., vaccination administered intranasally.

Citation: Qinhu Peng, Xiaohong Wu, Xingxing Li, Zelun Zhang, Hongshan Xu, Xinyu Liu, Wenjuan Li, Miao Li, Enyue Fang, Xiaohui Liu, Jingjing Liu, Danhua Zhao, Lihong Yang, Hongyu Wang, Jia Li, Yanqiu Huang, Leitai Shi, Yunpeng Wang, Ren Yang, Guangzhi Yue, Yue Suo, Min Li, Shouchun Cao, Qiang Ye and Yuhua Li. Heterologous Prime-boost with Chimpanzee Adenovirus Vector and Receptor-Binding Domain Recombinant Subunit Protein COVID-19 Vaccine Induces Strong Immune Responses in Mice. Archives of Microbiology and Immunology. 7 (2023): 408-420.

diluted serum was added to each well. Next, after washing with PBST six times again, the plates were subjected to 1-h incubation using horseradish peroxidase (HRP)-labeled goat anti-mouse IgA (Abcam, Cambridge, UK, 1:10,000) or IgG (ZSGB-BIO, Beijing, China, 1:10,000) at 37°C. Then, the plates were washed again, followed by the detection of antibody responses through absorbance values at 450/630 nm, separately, with 3,3',5,5'-tetramethylbenzidine (TMB) (Beyotime, Shanghai, China) being the substrate. Later, GraphPad Prism v9 was utilized to calculate serum IgA and IgG titers. We then determined the serum antibody titer by the reciprocal of greatest dilution, and it increased by 2.1 times compared with the absorbance of the negative control.

Recombinant vesicular stomatitis virus (VSV) pseudovirus-based neutralization test

The Division of HIV/AIDS and Sex-Transmitted Virus Vaccines of the National Institutes for Food and Drug Control offered recombinant VSV-based pseudotyped SARS-CoV-2, which included SARS-CoV-2 variants of Wuhan-Hu-1 together with Omicron (B.1.1.529). Mouse serum samples were first subjected to 30-min inactivation within a 56°C water bath diluted three-fold and mixed with 650 TCID₅₀ (50% tissue culture infectious dose) of VSV-based pseudovirus SARS-CoV-2 for 1-h incubation at 37°C. Later, we introduced 2 × 10⁵ Vero cells for another 24-h culture at 37°C with 5% CO₂. Moreover, luciferase activity was detected to determine the amount of pseudovirus entering the target cells, thus measuring the pseudovirus-neutralizing antibody (PNAb). The luciferase activity was detected using a luciferase assay system (PerkinElmer, Waltham, MA, USA). Every plate contained one virus control that contained the cells and virus alone, together with one negative control that contained the cells alone. For every sample, we determined the corresponding half-maximal effective concentration. With regard to the neutralizing titer < 30, its level was recorded as 30 prior to plotting.

Angiotensin-converting enzyme-2 (ACE2)-binding inhibition test (ELISA)

The titers of antibodies blocking ACE2 binding onto corresponding cognate ligands (spike proteins in Wuhan-Hu-1, B.1.1.7, B.1.351, B.1.526.1, B.1.617, B.1.617.1, B.1.617.2; AY.4, B.1.617.3, P.1 along with P.2 strains) were analyzed using the V-PLEX COVID-19 ACE2 neutralization kit (Meso Scale Discovery, Panel 18 [ACE2] kit, K15570U; Meso Scale Discovery (MSD), Rockville, MD, USA). Specifically, a specific antigen was coated onto the spots into a 96-well plate, followed by detection of antibodies bound within each sample (dilution: 1:100) using the MSD SULFO-TAG-conjugated human ACE2 protein. In this work, the MSD instrument for measuring light emission from the tag

was utilized for reading. We determined the ACE2-binding inhibition rate as follows:

$$\begin{aligned} \text{ACE2-binding inhibition rate} &= 1 - \frac{(\text{average electrochemiluminescence signal value of the sample} \\ &\quad - \text{average electrochemiluminescence signal value of the blank}) \times 100\%}{\text{average electrochemiluminescence signal value of the blank}} \end{aligned}$$

IFN-γ enzyme-linked immunospot (ELISpot) test

After euthanasia, each mouse was immersed in 75% ethanol. Mouse splenic tissue was dissected and placed in a 40-μm cell strainer that contained mouse lymphocyte separation medium (4–5 mL, Dakewe, Beijing, China), followed by grinding using a 2-mL syringe piston. Thereafter, the splenic cell suspension was added into the 15-mL centrifuge tube at once and coated using RPMI-1640 medium (1,000 μL, Hyclone, Logan, UT, USA), followed by 30-min centrifugation at 800 × g under ambient temperature. Afterwards, liquid within the centrifuge tube was classified as four layers from the top down, namely, RPMI-1640 medium, lymphocyte, fluid separation, as well as erythrocyte and cell fragment layers. Among them, the second layer was added to the new tube, followed by the addition of RPMI-1640 medium (10 mL). Meanwhile, after 10-min centrifugation at 250 × g and ambient temperature, lymphocytes were collected for suspension within the serum-free medium (Dakewe) after discarding the supernatants. Later, we employed the mouse IFN-γ ELISpot Plus kit (Mabtech, Stockholm, Sweden) for detecting IFN-γ-positive cells. To be specific, 1 × PBS (200 μL) was added to rinse the polyvinylidene fluoride-containing 96-well plates, followed by 2-h blocking using RPMI-1640 medium added with 10% fetal bovine serum at 24°C. Later, we introduced 2.5 × 10⁵ fresh lymphocytes into each well for another 24-h stimulation using the peptide pool (1 μg/mL/peptide; Genscript, Nanjing, China) produced by the peptide scan (15-mers with 11-residue overlaps) for the whole SARS-CoV-2 spike glycoprotein under 37°C and 5% CO₂ conditions. Then, anti-mouse IFN-γ antibody was added to incubate for a 2-h period under ambient temperature, followed by an additional 1-h incubation using streptavidin-HRP (dilution, 1:1,000; Dakewe). The cells were washed, and each well was introduced with TMB substrate solution (100 μL) for 5-min development until diverse spots occurred. The ImmunoSpot® S6 Universal instrument (Cellular Technology Limited, Shaker Heights, OH, USA) was employed for imaging and counting.

Intracellular cytokine staining

After isolation and stimulation of splenic lymphocytes using the peptide pool (2 μg/mL/peptide) produced by the peptide scan (15-mers with 11-residue overlaps) for the whole SARS-CoV-2 spike glycoprotein, cytokine production was blocked by 6-h incubation using the spike protein peptide pool (2 μg/mL) as well as brefeldin A (dilution, 1:1,000; Biolegend, San Diego, CA, USA) at 37°C and 5% CO₂. After

washing, the splenocytes were subjected to staining using the antibody mixture consisting of the BV421 hamster anti-mouse CD3e antibody, FITC rat anti-mouse CD8a antibody, BV510 rat anti-mouse CD4 antibody, and fixable viability stain 780 (all from BD Biosciences, San Jose, CA, USA) for excluding dead cells. Cells were then washed twice using $1 \times$ PBS, followed by fixation and permeabilization using Cytotfix/Cytoperm (BD Biosciences), washing by Perm/Wash buffer (BD Biosciences), then staining using PE-labeled rat anti-mouse IFN- γ , BV605 rat anti-mouse IL-2, PE-Cy7 rat anti-mouse IL-4, APC rat anti-mouse IL-10, together with BB700 rat anti-mouse tumor necrosis factor (TNF) (BD Biosciences). After successive washing by Perm/Wash buffer, the cells were subjected to resuspension within $1 \times$ PBS prior to flow cytometric analysis with the FACS Lyric analyzer (BD Biosciences). There were 200,000 events or more obtained in every sample. FlowJo software (TreeStar, Ashland, OR, USA) was applied for the data analysis. CD4⁺ and CD8⁺ T cells were gated from lymphocytes (FSC-A versus SSC-A), single cells (FSC-A versus FSC-H), as well as living CD3⁺ T cells (CD3⁺ versus LD780⁻). The data were represented by cytokine-positive cell proportions of CD4⁺ or CD8⁺ T cells.

MSD Th1/Th2 cytokine analysis

We obtained supernatants in the ELISpot plates to analyze TNF- α and IL-2/-4/-10 levels with the V-PLEX Proinflammatory Panel 1 (mouse) Kit (Meso Scale Discovery), in line with the manufacturer's instructions. Cytokines were analyzed using MESO QuickPlex SQ 120 (Meso Scale Discovery), after which we adopted the standard curve for measuring their levels.

Statistical analysis

This work utilized GraphPad Prism v9 software for graph and statistical analyses. The results were represented by geometric mean \pm geometric standard deviation (SD). One-way analysis of variance (ANOVA) was applied to analyze statistical differences across the groups. $p < 0.05$ stood for statistical significance (* $p < 0.05$; ** $p < 0.01$; *** $p < 0.001$; **** $p < 0.0001$; ns, no significant differences).

Results

Heterologous prime-boost with ChAd and ZF2001 induced strong mouse humoral immunity

Fig. 1A and 1B display heterologous prime-boost designs. This work measured spike protein-specific IgG and IgA, as well as pseudoviral neutralizing antibody titers, to evaluate humoral immune response levels. ELISA was conducted to detect spike protein-specific IgG and IgA titers (Fig. 2), which are shown in Fig. 2A and 2B, respectively, at 14 days following primary immunization. As shown in Fig. 1A, compared to single-dose i.m. administration of ZF2001,

single-dose i.n. or i.m. administration of ChAd triggered higher spike-specific IgG titers. The i.n. ChAd administration at one individual dose triggered spike-specific IgA (Fig. 1B), with no significant differences between all vaccination groups. Spike-specific IgG titers of each group at 42 days following primary immunization are shown in Fig. 2C. The i.m. administration groups i.m. ChAd > i.m. ZF2001, i.m. ZF2001 > i.m. ChAd, i.m. ZF2001+ChAd, $1 \times$ i.m. ChAd, $2 \times$ i.m. ChAd, and $2 \times$ i.m. ZF2001) had slightly higher IgG titer levels compared to the i.n. ChAd administration groups (i.n. ChAd > i.m. ZF2001, i.m. ZF2001 > i.n. ChAd, $1 \times$ i.n. ChAd, and $2 \times$ i.n. ChAd), where the i.m. ChAd > i.m. ZF2001 group exhibited the greatest IgG geometric mean neutralizing antibody titers (GMTs) of 507835, which were 3.82-, 2.10-, 9.10-, and 7.05-fold higher compared to the i.n. administration groups (i.n. ChAd > i.m. ZF2001, i.m. ZF2001 > i.n. ChAd, $1 \times$ i.n. ChAd, and $2 \times$ i.n. ChAd, respectively). The i.n. ChAd administration groups (i.n. ChAd > i.m. ZF2001, i.m. ZF2001 > i.n. ChAd, $1 \times$ i.n. ChAd, and $2 \times$ i.n. ChAd) developed the highest level of spike-specific IgA titers at 42 days following primary immunization (Fig. 2D). The i.n. ChAd > i.m. ZF2001, i.m. ZF2001 > i.n. ChAd, $1 \times$ i.n. ChAd, and $2 \times$ i.n. ChAd groups induced IgA GMTs of 784, 494, 1005, and 931, respectively.

A VSV-based pseudovirus assay was conducted to assess virus-specific PNAb titers in the serum to resist the Wuhan-Hu-1 strain (Fig. 3A) together with the B.1.1.529 (Fig. 3B) variant at 42 days following primary immunization. As shown in Fig. 3A, the i.m. administration of ZF2001 groups (i.n. ChAd > i.m. ZF2001, i.m. ZF2001 > i.n. ChAd, i.m. ChAd > i.m. ZF2001, i.m. ZF2001 > i.m. ChAd, i.m. ZF2001+ChAd, and $2 \times$ i.m. ZF2001) to the Wuhan-Hu-1 strain of the pseudovirus developed relatively high PNAb GMTs, which did not show any significant difference between the groups. Herein, i.m. ChAd > i.m. ZF2001 induced the highest response against the Wuhan-Hu-1 strain PNAb titers, with a PNAb GMT of 11358. Fig. 3B shows the virus-specific serum PNAb titers in mouse serum to resist the B.1.1.529 variant on day 42 after primary immunization. Ten vaccination groups induced different decreases in PNAb titers in comparison with the Wuhan-Hu-1 strain. The $2 \times$ i.n. ChAd group triggered the greatest PNAb titers, and the PNAb GMT was 302. The heterologous prime-boost immunization groups (i.n. ChAd > i.m. ZF2001, i.m. ZF2001 > i.n. ChAd, i.m. ChAd > i.m. ZF2001, i.m. ZF2001 > i.m. ChAd, and i.m. ZF2001+ChAd) had PNAb GMTs of 56, 188, 69, 108, and 120, respectively. The $2 \times$ i.n. ChAd group had 5.39-, 1.61-, 4.38-, 2.80-, and 2.52-fold higher PNAb GMTs compared to the heterologous prime-boost groups (i.n. ChAd > i.m. ZF2001, i.m. ZF2001 > i.n. ChAd, i.m. ChAd > i.m. ZF2001, i.m. ZF2001 > i.m. ChAd, and i.m. ZF2001+ChAd, respectively).

Heterologous prime-boost using ChAd and ZF2001 induced broad-spectrum neutralizing activity against various SARS-CoV-2 variants within mice

ACE2-binding inhibition (neutralization) ELISA was conducted to evaluate ACE2-binding inhibition (neutralizing activity) of spike proteins from different strains (Wuhan-Hu-1, B.1.1.7, B.1.351, B.1.526.1, B.1.617, B.1.617.1, B.1.617.2; AY.4, B.1.617.3, P.1, as well as P.2) in serum at 42 days following primary immunization, for assessing broad-spectrum neutralizing activities (Fig. 4 A–F).

Strategies of i.m. ZF2001 > i.n. ChAd, i.m. ChAd > i.m. ZF2001 and 2 × i.m. ZF2001 induced comparable levels of ACE2-binding inhibition rates. Among these, i.m. ZF2001 > i.n. ChAd was the highest, and the ACE2-binding inhibition rates against Wuhan-Hu-1, B.1.1.7, B.1.351, B.1.526.1, B.1.617, B.1.617.1, B.1.617.2; AY.4, B.1.617.3, P.1, together with P.2 were 99%, 97%, 85%, 96%, 94%, 94%, 96%, 95%, 83%, and 88%, respectively. The 1 × i.n. ChAd, 2 × i.n. ChAd, 1 × i.m. ChAd, and 2 × i.m. ChAd combinations

induced relatively low ACE2-binding inhibition rates. The inhibition rate arithmetic mean values (AMVs) for these four groups against Wuhan-Hu-1, B.1.1.7, B.1.351, B.1.526.1, B.1.617, B.1.617.1, B.1.617.2; AY.4, B.1.617.3, P.1, and P.2 were all in the range of 20–51%.

Heterogeneous prime-boost with ChAd and ZF2001 induced cellular immunity to resist SARS-CoV-2 within mice

Mouse splenic lymphocytes were harvested 56 days following primary immunization, followed by 24-h stimulation using the peptide pools that spanned the Wuhan-Hu-1 spike proteins, followed by IFN-γ ELISpot assays (Fig. 5). The i.m. ChAd administration groups (i.m. ZF2001 > i.m. ChAd, i.m. ChAd > i.m. ZF2001, i.m. ZF2001+ChAd, 1 × i.m. ChAd, and 2 × i.m. ChAd) induced significantly higher IFN-γ than the i.n. ChAd administration groups (i.n. ChAd > i.m. ZF2001, i.m. ZF2001 > i.n. ChAd, 1 × i.n. ChAd and 2 × i.n. ChAd). Among all experimental groups, the i.m. ZF2001 > i.m. ChAd group induced the highest T cell

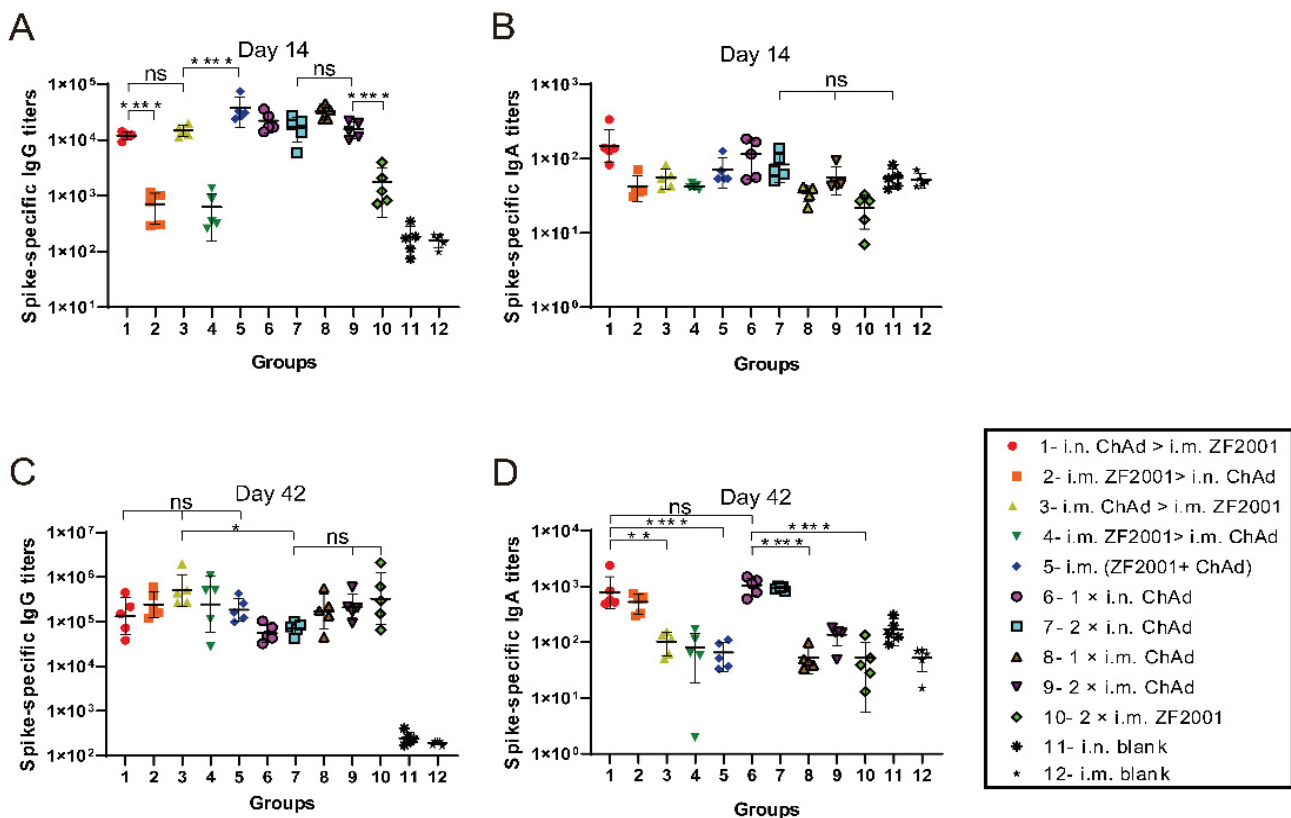


Figure 2: Humoral immunity is triggered via different administration routes of ZF2001 and ChAdTS-S. Spike-specific IgG and IgA titers were measured on days 14 and 42 after primary immunization. (A) Spike-specific IgG titers in the serum 14 days following primary immunization (n = 5 for each group, with one point indicating a sample). (B) Serum spike-specific IgA titers 14 days following primary immunization (n = 5 for each group, with one point indicating a sample). (C) Serum spike-specific IgG titers 42 days following primary immunization (n = 5 for each group, with one point indicating a sample). (D) Spike-specific IgA titers in the serum 42 days following primary immunization (n = 5 for each group, with one point indicating a sample). Bars indicate geometric mean ± geometric SD; *p < 0.05; **p < 0.01; ****p < 0.0001; ns, no significant differences

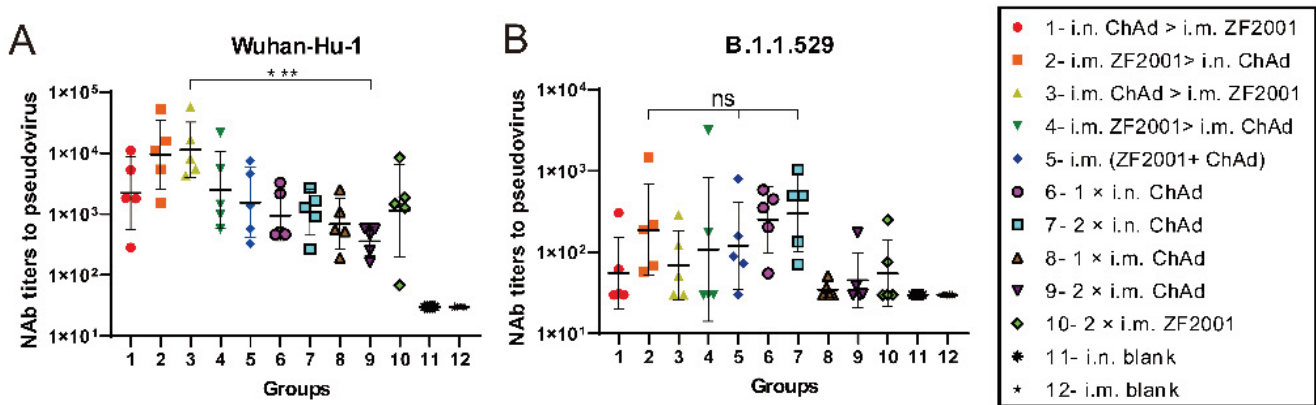


Figure 3: Virus-specific PNAb titers in the serum to resist the Wuhan-Hu-1 strain together with the B.1.1.529 variant accessed by VSV-based pseudovirus assays 42 days following primary immunization. PNAb in the serum to resist (A) Wuhan-Hu-1 and (B) B.1.1.529; bars indicate geometric mean \pm geometric SD. *** $p < 0.001$; ns: $p > 0.05$.

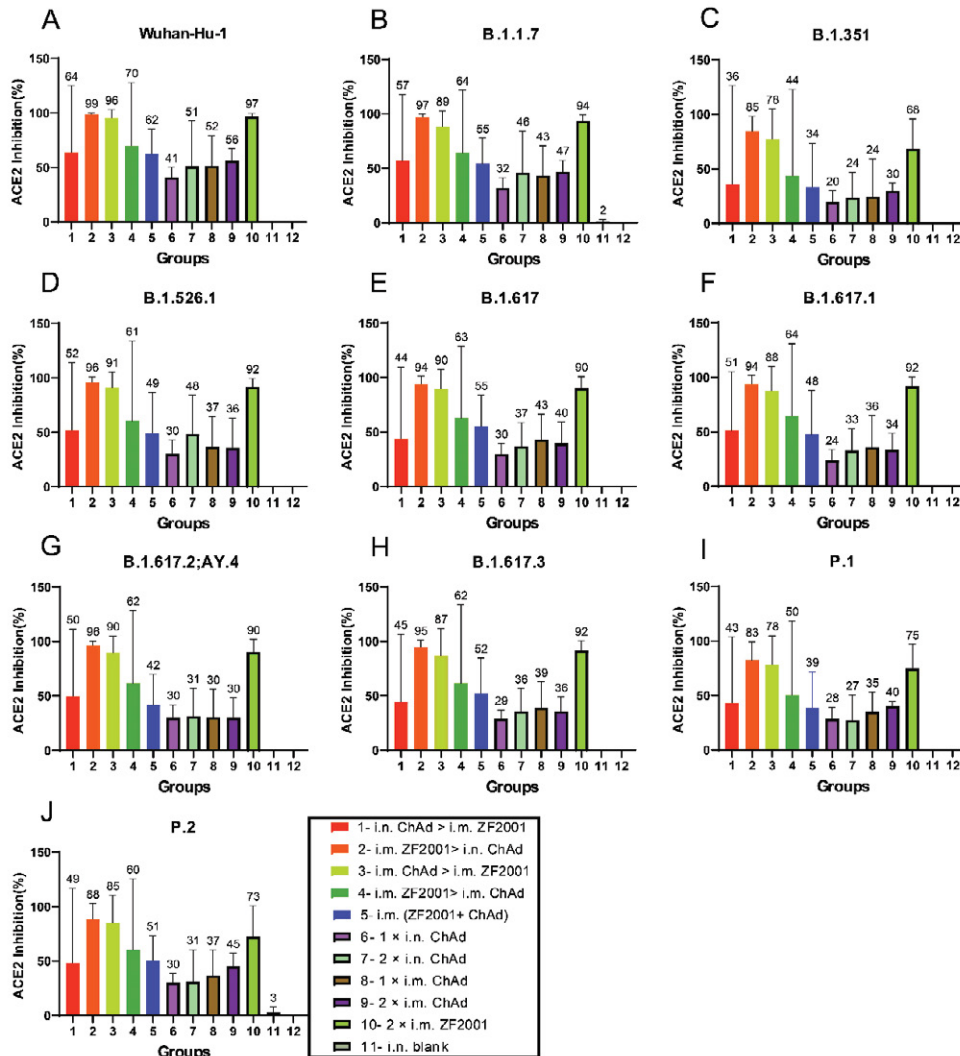


Figure 4: The neutralization activity of the serum was analyzed by determining ACE2-binding inhibition to SARS-CoV-2 spike proteins at 42 days following primary immunization. The serum neutralizing activity in ACE2-binding inhibition to SARS-CoV-2 spike proteins in (A) Wuhan-Hu-1, (B) B.1.1.7, (C) B.1.351, (D) B.1.526.1, (E) B.1.617, (F) B.1.617.1, (G) B.1.617.2; AY.4, (H) B.1.617.3, (I) P.1, and (J) P.2) was determined at 42 days following primary immunization. The negative ACE2-binding inhibition rate is represented by zero ($n = 5$ for each group). Bars indicate mean \pm SD, and each number indicates the geometric mean of the corresponding group.

Citation: Qinhua Peng, Xiaohong Wu, Xingxing Li, Zelun Zhang, Hongshan Xu, Xinyu Liu, Wenjuan Li, Miao Li, Enyue Fang, Xiaohui Liu, Jingjing Liu, Danhua Zhao, Lihong Yang, Hongyu Wang, Jia Li, Yanqiu Huang, Leitai Shi, Yunpeng Wang, Ren Yang, Guangzhi Yue, Yue Suo, Min Li, Shouchun Cao, Qiang Ye and Yuhua Li. Heterologous Prime-boost with Chimpanzee Adenovirus Vector and Receptor-Binding Domain Recombinant Subunit Protein COVID-19 Vaccine Induces Strong Immune Responses in Mice. Archives of Microbiology and Immunology. 7 (2023): 408-420.

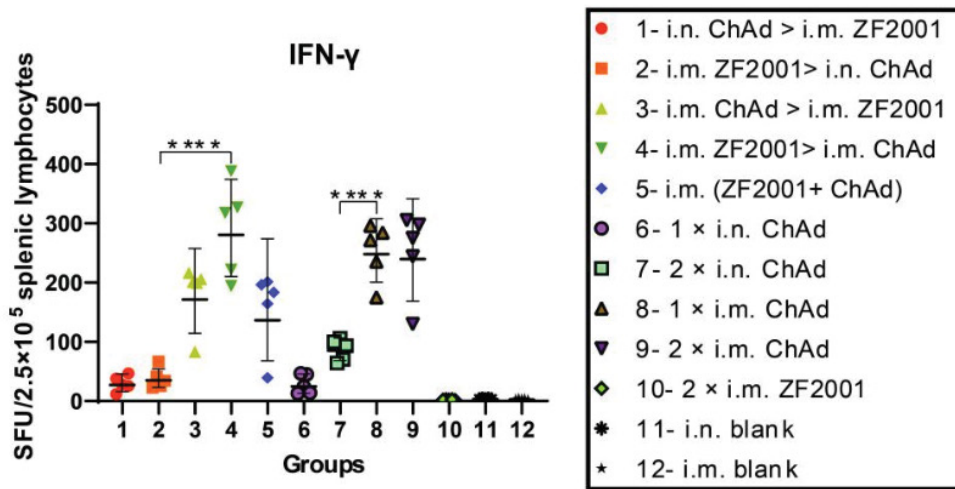


Figure 5: SARS-CoV-2 spike protein-specific cellular immunity was determined on day 56 following primary immunization. ELISpot assays were conducted to determine the IFN- γ levels after SARS-CoV-2 spike protein stimulation. After euthanasia of five animals from each group, we determined T cell responses. Later, Wuhan-Hu-1 spike peptide pools that spanned the whole spike protein sequence were adopted in lymphocyte stimulation. ELISpot assays were then performed to quantify cells secreting IFN- γ ($n = 5$ for each group, with one point indicating the mean of spots in two wells of each sample). Bars indicate geometric mean \pm geometric SD. **** $p < 0.0001$; ns: $p > 0.05$. SFUs, spot-forming units.

responses, and the GMT of spot-forming units (SFUs) was 281 for every 2.5×10^5 splenic lymphocytes. Other heterologous prime-boost groups (i.n. ChAd > i.m. ZF2001, i.m. ZF2001 > i.n. ChAd, i.m. ChAd > i.m. ZF2001, and i.m. ZF2001+ChAd) had relatively low T cell responses, and the GMTs of SFUs were 27, 35, 172, and 136, respectively, for every 2.5×10^5 splenic lymphocytes, which were 10.41-, 8.03-, 1.63-, 1.63-, and 2.07-fold lower, respectively, compared to those of the i.m. ZF2001 > i.m. ChAd group.

Heterogenic prime-boost with ChAd and ZF2001 skewed the T cell response

This study harvested splenic lymphocytes at 56 days following primary immunization, followed by stimulation using the overlapping spike protein peptide pool to assess the Th1 dominance in spike-specific T cell responses. The Th1-biased T cell responses against SARS-CoV-2 were analyzed by the MSD cytokine profiling assay and intracellular cytokine staining. Fig. 6A–J indicates the results of intracellular cytokine staining, where i.m. administration of ChAd induced a higher Th1 response.

For every vaccination group, the i.m. ChAd administration groups (i.m. ZF2001 > i.m. ChAd, i.m. ChAd > i.m. ZF2001, i.m. ZF2001+ChAd, 1 \times i.m. ChAd, and 2 \times i.m. ChAd) were significantly increased compared to the other vaccination groups (i.m. ZF2001 > i.n. ChAd, i.n. ChAd > i.m. ZF2001, 1 \times i.n. ChAd, 2 \times i.n. ChAd and 2 \times i.m. ZF2001) in the CD4+/CD8+ T cell ratio (%), secreting Th1 cytokines (IFN- γ , TNF- α , and IL-2). The CD4+/CD8+ T cell ratio that

secreted Th2 cytokines (IL-4 and IL-10) did not show any significant difference in the heterologous prime-boost relative to homologous prime-boost immunization groups. TNF- α and IL-2/-4/-5/-6/-10-specific MSD cytokine profiling assays (Fig. 7A–F) were carried out to assess functional preservation together with polarization in spike protein-specific T cells against the Wuhan-Hu-1 strain. For every experimental group, i.m. ChAd administration groups i.m. ZF2001 > i.m. ChAd, i.m. ChAd > i.m. ZF2001, i.m. ZF2001+ChAd, 1 \times i.m. ChAd, and 2 \times i.m. ChAd) elicited increased IL-2 and TNF- α contents, where the 2 \times i.m. ChAd group induced the highest concentrations. However, the secretion of IL-4/-5/-6/-10 decreased and was comparable to the i.n. and i.m. blank groups. The above results suggest that i.m. administration of ChAd increases the Th1-biased response rather than the Th2-biased counterpart.

Discussion

The emergence of Omicron variants has raised concerns about vaccine efficacy, and it has become particularly important to explore proven immunization strategies [33]. Jin et al. [34] administered a heterologous booster with ZF2001 in adults receiving one individual dose of Convidecia with no SARS-CoV-2 infection. According to these results, the heterologous prime-boost induced higher immunogenicity compared with single-dose Convidecia administration, and there were no safety concerns. In the present study, i.m. ChAd > i.m. ZF2001 triggered the greatest IgG and PNAbs titers, higher ACE2-binding inhibition rates, and a Th1-skewed response against SARS-CoV-2.

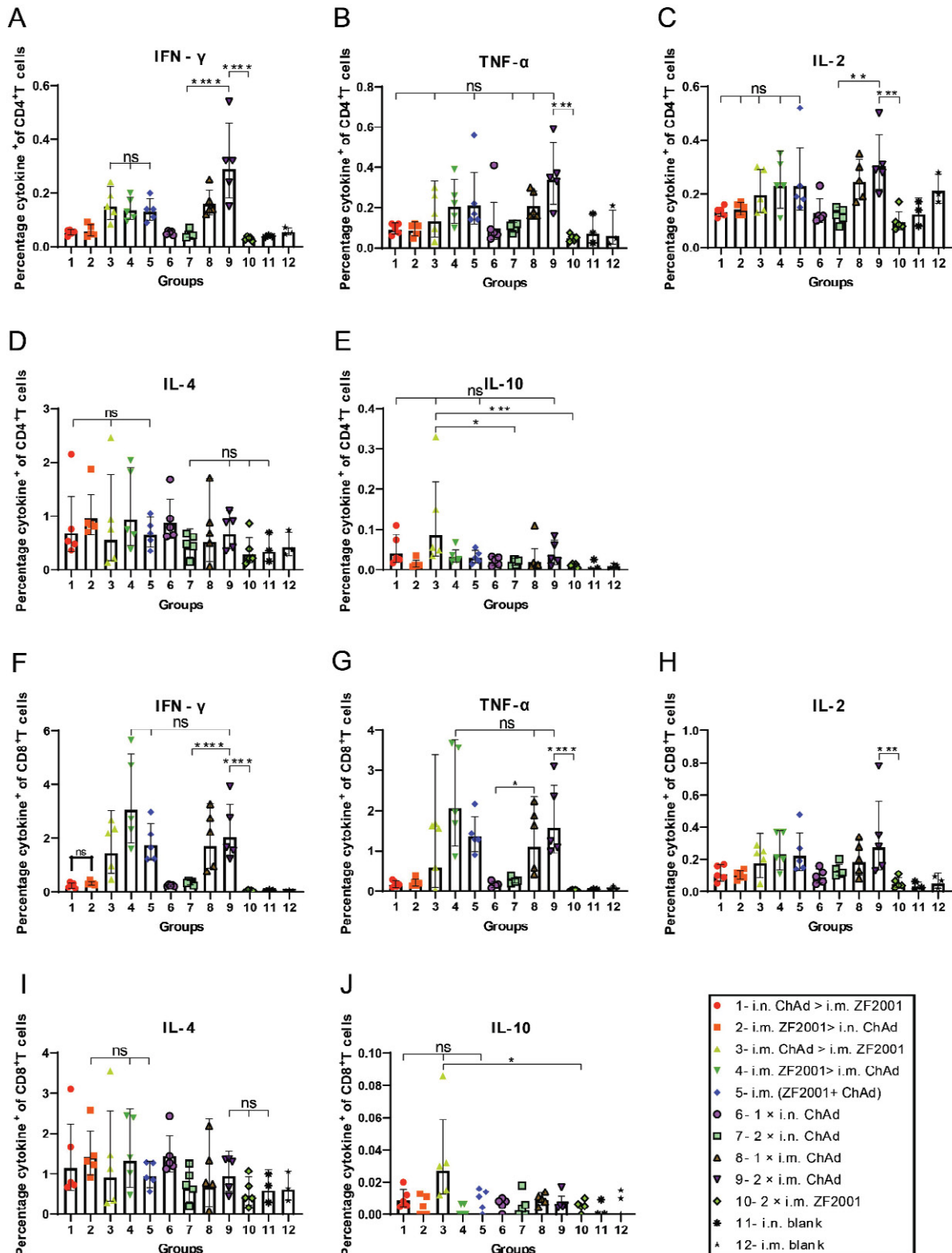


Figure 6: Th1/Th2 imbalance was determined by intracellular cytokine staining 56 days following primary immunization. The spike protein-specific TNF- α -, IFN- γ -, and IL-2/-4/-10-positive memory (A-E) CD4+ T together with (F-J) CD8+ T cell percentages were determined 56 days following primary immunization (n = 4 for each group, with one point indicating a sample). Bars indicate geometric mean \pm geometric SD. *p < 0.05; ***p < 0.001; ****p < 0.0001; ns: p > 0.05.

Citation: Qinhu Peng, Xiaohong Wu, Xingxing Li, Zelun Zhang, Hongshan Xu, Xinyu Liu, Wenjuan Li, Miao Li, Enyue Fang, Xiaohui Liu, Jingjing Liu, Danhua Zhao, Lihong Yang, Hongyu Wang, Jia Li, Yanqiu Huang, Leitai Shi, Yunpeng Wang, Ren Yang, Guangzhi Yue, Yue Suo, Min Li, Shouchun Cao, Qiang Ye and Yuhua Li. Heterologous Prime-boost with Chimpanzee Adenovirus Vector and Receptor-Binding Domain Recombinant Subunit Protein COVID-19 Vaccine Induces Strong Immune Responses in Mice. Archives of Microbiology and Immunology. 7 (2023): 408-420.

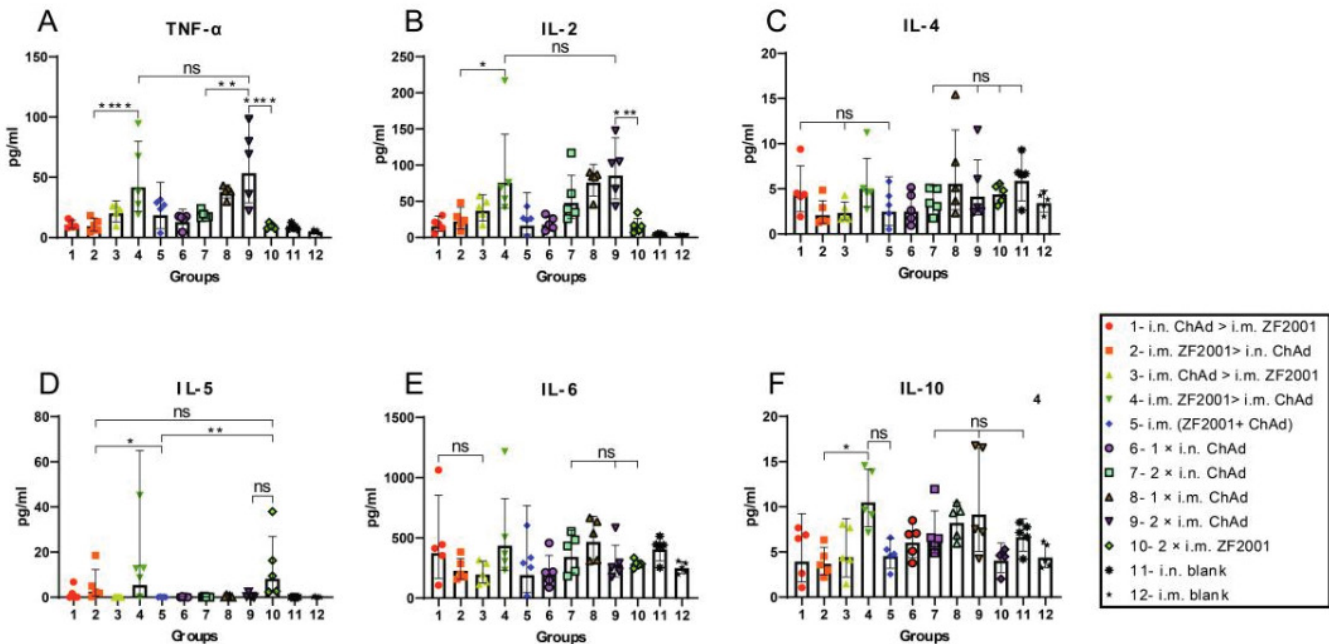


Figure 7: Th1/Th2 imbalance within immunized mice was determined by MSD cytokine profiling. Wuhan-Hu-1 spike peptide pools that spanned the whole spike protein sequence were added for 24-h lymphocyte stimulation. Supernatant contents of TNF- α and IL-2/-4/-5/-6/-10 were determined (n = 5 for each group, with every point representing a sample). Bars stand for geometric mean \pm geometric SD. *p < 0.05; **p < 0.01; ***p < 0.001; ****p < 0.0001; ns, p > 0.05.

Our results demonstrated that i.n. administration of ChAd produced higher levels of IgA than i.m. administration. This result may be related to the induction of secretory IgA (sIgA) production by nasopharyngeal-associated lymphoid tissues, and these produced sIgAs are mainly present in secretions [35–37]. sIgA achieves neutralization by combining with SARS-CoV-2’s receptor-binding domain (RBD) [38,39]. sIgA produced by mucosal immune induction has a critical effect on neutralizing SARS-CoV-2 during early infection, as well as in defense against infection [39,40]. The neutralizing antibody levels produced to resist the B.1.1.529 strain ranged from 3.75–164.61-fold, which decreased relative to those produced to resist the Wuhan-Hu-1 strain. Reynolds et al. [41] examined serum levels of PNAbs produced to resist diverse SARS-CoV-2 variants among healthcare workers receiving three BNT162b2 vaccine doses. Consequently, compared to other VOC, the BNT162b2 vaccine produced significantly reduced PNAbs to resist B.1.1.529. This result is due to many variant sites and base-pair deletions on the spike protein of the B.1.1.529 strain, preventing antibodies from recognizing some of the spike proteins effectively, resulting in a strong humoral immune escape of the Omicron strain [42]. K417N and E484A on the RBD are considered the main causes of the immune escape of B.1.1.529 [42,43].

In this study, the i.m. administration of ZF2001 induced lower levels of T cell immune responses. In a phase I/II clinical trial enrolling healthy adults aged 18–59 years, Yang

et al. [44] tested the induction of lower IFN- γ and IL-2/-4/-5 cytokine levels following immunization using 25 or 50 μ g of a three-dose ZF2001 vaccine. Their findings were consistent with ours. However, higher levels of T cell immunity were attributed to i.m. injection of ChAdTS-S. Li et al. [45] found that i.m. administration of single or double doses of ChAdTS-S to mice induced higher levels of T cell immune responses compared with blank controls, as was shown in our study. Moreover, the heterologous prime-boost with ZF2001 and ChAdTS-S produced a higher Th1 response compared to the homologous prime-boost with ZF2001.

Our study has many shortcomings. First, due to resource limitations, we only detected neutralizing antibodies to resist Wuhan-Hu-1 as well as B.1.1.529 pseudoviruses at the neutralizing antibody level, and further research using more VOC is needed. Neutralizing antibodies play a critical role in protecting against SARS-CoV-2 [46]. As neutralizing antibodies against live viruses were not detected, this is one of the shortcomings of this paper. Second, we only measured antibody levels in serum to detect IgA, and antibody levels in lung lavage fluid were not further tested, which should be addressed in future work. Third, the assays of cellular immunity performed in this study were based on the Wuhan-Hu-1 strain. To further investigate broad-spectrum immune effects produced by different vaccination methods, more VOC should be used.

Conclusion

ChAdTS-S, a heterologous strategy based on the chimpanzee adenovirus vector vaccine, together with ZF2001, the recombinant subunit vaccine, can not only reduce infection in a living body infected with multiple SARS-CoV-2 variants but also induce higher levels of neutralizing antibody titers, as well as higher cellular immunity compared to a homologous prime-boost strategy. Thus, it can be used as an immunoprophylactic approach to deal with emerging variants and to lay a foundation for exploring novel immunization strategies.

Acknowledgements

We would like to thank Walvax Biotechnology Co., Ltd. for providing the ChAdTS-S vaccine, Anhui Zhifei Longcom Biopharmaceutical Co., Ltd. for providing the ZF2001 vaccine, and Editage (www.Editage.cn) for English language editing.

References

- Cele S, Jackson L, Khoury DS, Khan K, Moyo-Gwete T, Tegally H, et al. Omicron extensively but incompletely escapes Pfizer BNT162b2 neutralization. *Nature* 602 (2022): 654–656.
- Liu C, Ginn HM, Dejnirattisai W, Supasa P, Wang B, Tuekprakhon A, et al. Reduced neutralization of SARS-CoV-2 B.1.617 by vaccine and convalescent serum. *Cell* 184 (2021): 4220–4236.
- Wang P, Nair MS, Liu L, Iketani S, Luo Y, Guo Y, et al. Antibody resistance of SARS-CoV-2 variants B.1.351 and B.1.1.7. *Nature* 593 (2021): 130–135.
- Hoffmann M, Arora P, Groß R, Seidel A, Hörmich BF, Hahn AS, et al. SARS-CoV-2 variants B.1.351 and P.1 escape from neutralizing antibodies. *Cell* 184 (2021): 2384–2393.
- Shen X, Tang H, Pajon R, Smith G, Glenn GM, Shi W, et al. Neutralization of SARS-CoV-2 variants B.1.429 and B.1.351. *N Engl J Med* 384 (2021): 2352–2354.
- World Health Organization. WHO Coronavirus (COVID-19) Dashboard. Internet (2023).
- Madhi SA, Baillie V, Cutland CL, Voysey M, Koen AL, Fairlie L, et al. Efficacy of the ChAdOx1 nCoV-19 Covid-19 vaccine against the B.1.351 Variant. *N Engl J Med* 384 (2021): 1885–1898.
- Nanduri S, Pilishvili T, Derado G, Soe MM, Dollard P, Wu H, et al. Effectiveness of Pfizer-BioNTech and Moderna vaccines in preventing SARS-CoV-2 infection among nursing home residents before and during widespread circulation of the SARS-CoV-2 B.1.617.2 (Delta) variant – National Healthcare Safety Network, March 1–August 1, 2021. *MMWR Morb Mortal Wkly Rep* 70 (2021): 1163–1166.
- Shinde V, Bhikha S, Hoosain Z, Archary M, Bhorat Q, Fairlie L, et al. Efficacy of NVX-CoV2373 Covid-19 vaccine against the B.1.351 Variant. *N Engl J Med* 384 (2021): 1899–1909.
- Vacharathit V, Aiewsakun P, Manopwisedjaroen S, Srisaowakarn C, Laopanupong T, Ludowyke N, et al. CoronaVac induces lower neutralising activity against variants of concern than natural infection. *Lancet Infect Dis* 21 (2021): 1352–1354.
- Chang J. Adenovirus vectors: excellent tools for vaccine development. *Immune Netw* 21 (2021): e6.
- Guo J, Mondal M, Zhou D. Development of novel vaccine vectors: chimpanzee adenoviral vectors. *Hum Vaccin Immunother* 14 (2018): 1679–1685.
- Zhang S, Huang W, Zhou X, Zhao Q, Wang Q, Jia B. Seroprevalence of neutralizing antibodies to human adenoviruses type-5 and type-26 and chimpanzee adenovirus type-68 in healthy Chinese adults. *J Med Virol* 85 (2013): 1077–1084.
- Jia W, Channappanavar R, Zhang C, Li M, Zhou H, Zhang S, et al. Single intranasal immunization with chimpanzee adenovirus-based vaccine induces sustained and protective immunity against MERS-CoV infection. *Emerg Microbes Infect* 8 (2019): 760–772.
- Li M, Guo J, Lu S, Zhou R, Shi H, Shi X, et al. Single-dose immunization with a chimpanzee adenovirus-based vaccine induces sustained and protective immunity against SARS-CoV-2 infection. *Front Immunol* 12 (2021): 697074.
- Lu M, Liu K, Peng Y, Ding Z, Li Y, Tendu A, et al. Recombinant chimpanzee adenovirus vector vaccine expressing the spike protein provides effective and lasting protection against SARS-CoV-2 infection in mice. *Virology* 537 (2022): 581–590.
- Ramasamy MN, Minassian AM, Ewer KJ, Flaxman AL, Folegatti PM, Owens DR, et al. Safety and immunogenicity of ChAdOx1 nCoV-19 vaccine administered in a prime-boost regimen in young and old adults (COV002): a single-blind, randomised, controlled, phase 2/3 trial. *Lancet* 396 (2020): 1979–1993.
- Folegatti PM, Ewer KJ, Aley PK, Angus B, Becker S, Belij-Rammerstorfer S, et al. Safety and immunogenicity of the ChAdOx1 nCoV-19 vaccine against SARS-CoV-2: a preliminary report of a Phase 1/2, single-blind, randomised controlled trial. *Lancet* 396 (2020): 467–478.

19. Andrews N, Stowe J, Kirsebom F, Toffa S, Rickeard T, Gallagher E, et al. Covid-19 vaccine effectiveness against the omicron (B.1.1.529) variant. *N Engl J Med* 386 (2022): 1532–1546.
20. Wu S, Zhong G, Zhang J, Shuai L, Zhang Z, Wen Z, et al. A single dose of an adenovirus-vectored vaccine provides protection against SARS-CoV-2 challenge. *Nat Commun* 11 (2020): 4081.
21. Bricker TL, Darling TL, Hassan AO, Harastani HH, Soung A, Jiang X, et al. A single intranasal or intramuscular immunization with chimpanzee adenovirus-vectored SARS-CoV-2 vaccine protects against pneumonia in hamsters. *Cell Rep* 36 (2021): 109400.
22. Hassan AO, Kafai NM, Dmitriev IP, Fox JM, Smith BK, Harvey IB, et al. A single-dose intranasal ChAd vaccine protects upper and lower respiratory tracts against SARS-CoV-2. *Cell* 183 (2020): 169–184.
23. Dai L, Gao L, Tao L, Hadinegoro SR, Erkin M, Ying Z, et al. Efficacy and safety of the RBD-dimer-based Covid-19 vaccine ZF2001 in adults. *N Engl J Med* 386 (2022): 2097–2111.
24. Sacks HS. The Novavax vaccine had 90% efficacy against COVID-19 ≥ 7 d after the second dose. *Ann Intern Med* 174 (2021): JC124.
25. Bian L, Bai Y, Gao F, Liu M, He Q, Wu X, et al. Effective protection of ZF2001 against the SARS-CoV-2 Delta variant in lethal K18-hACE2 mice. *Virology* 19 (2022): 86.
26. Zhao X, Zheng A, Li D, Zhang R, Sun H, Wang Q, et al. Neutralisation of ZF2001-elicited antisera to SARS-CoV-2 variants. *Lancet Microbe* 2 (2021): e494.
27. Zhao X, Zhang R, Qiao S, Wang X, Zhang W, Ruan W, et al. Omicron SARS-CoV-2 neutralization from inactivated and ZF2001 vaccines. *N Engl J Med* 387 (2022): 277–280.
28. He Q, Mao Q, an C, Zhang J, Gao F, Bian L, et al. Heterologous prime-boost: breaking the protective immune response bottleneck of COVID-19 vaccine candidates. *Emerg Microbes Infect* 10 (2021): 629–637.
29. Tarke A, Coelho CH, Zhang Z, Dan JM, Yu ED, Methot N, et al. SARS-CoV-2 vaccination induces immunological T cell memory able to cross-recognize variants from Alpha to Omicron. *Cell* 185 (2022): 847–859.
30. Li W, Li X, Zhao D, Liu J, Wang L, Li M, et al. Heterologous prime-boost with AdC68- and mRNA-based COVID-19 vaccines elicit potent immune responses in mice. *Signal Transduct Target Ther* 6 (2021): 419.
31. Tenbusch M, Schumacher S, Vogel E, Priller A, Held J, Steininger P, et al. Heterologous prime-boost vaccination with ChAdOx1 nCoV-19 and BNT162b2. *Lancet Infect Dis* 21 (2021): 1212–1213.
32. Atmar RL, Lyke KE, Deming ME, Jackson LA, Branche AR, El Sahly HM, et al. Homologous and heterologous Covid-19 booster vaccinations. *N Engl J Med* 386 (2022): 1046–1057.
33. Zuo F, Abolhassani H, Du L, Piralla A, Bertoglio F, de Campos-Mata L, et al. Heterologous immunization with inactivated vaccine followed by mRNA-booster elicits strong immunity against SARS-CoV-2 Omicron variant. *Nat Commun* 13 (2022): 2670.
34. Jin P, Guo X, Chen W, Ma S, Pan H, Dai L, et al. Safety and immunogenicity of heterologous boost immunization with an adenovirus type-5-vectored and protein-subunit-based COVID-19 vaccine (Convdecia/ZF2001): A randomized, observer-blinded, placebo-controlled trial. *PLOS Med* 19 (2022): e1003953.
35. Underdown BJ, Schiff JM. Immunoglobulin A: strategic defense initiative at the mucosal surface. *Annu Rev Immunol* 4 (1986): 389–417.
36. Koshland ME. The coming of age of the immunoglobulin J chain. *Annu Rev Immunol* 3 (1985): 425–453.
37. Pabst O. New concepts in the generation and functions of IgA. *Nat Rev Immunol* 12 (2012): 821–832.
38. Ma H, Zeng W, He H, Zhao D, Jiang D, Zhou P, et al. Serum IgA, IgM, and IgG responses in COVID-19. *Cell Mol Immunol* 17 (2020): 773–775.
39. Sterlin D, Malaussena A, Gorochov G. IgA dominates the early neutralizing antibody response to SARS-CoV-2 virus [IgA dominates the early neutralizing antibody response to SARS-CoV-2 virus]. *Med Sci (Paris)* 37 (2021): 968–970.
40. Fröberg J, Diavatopoulos DA. Mucosal immunity to severe acute respiratory syndrome coronavirus 2 infection. *Curr Opin Infect Dis* 34 (2021): 181–186.
41. Reynolds CJ, Pade C, Gibbons JM, Otter AD, Lin KM, Muñoz Sandoval D, et al. Immune boosting by B.1.1.529 (Omicron) depends on previous SARS-CoV-2 exposure. *Science* 377 (2022).
42. Chen J, Wang R, Gilby NB, Wei GW. Omicron variant (B.1.1.529): infectivity, vaccine breakthrough, and antibody resistance. *J Chem Inf Model* 62 (2022): 412–422.
43. Tiecco G, Storti S, Degli Antoni M, Focà E, Castelli F, Quiros-Roldan E. Omicron genetic and clinical peculiarities that may overturn SARS-CoV-2 pandemic: a literature review. *Int J Mol Sci* 23 (2022): 1987.

Citation: Qinhua Peng, Xiaohong Wu, Xingxing Li, Zelun Zhang, Hongshan Xu, Xinyu Liu, Wenjuan Li, Miao Li, Enyue Fang, Xiaohui Liu, Jingjing Liu, Danhua Zhao, Lihong Yang, Hongyu Wang, Jia Li, Yanqiu Huang, Leitai Shi, Yunpeng Wang, Ren Yang, Guangzhi Yue, Yue Suo, Min Li, Shouchun Cao, Qiang Ye and Yuhua Li. Heterologous Prime-boost with Chimpanzee Adenovirus Vector and Receptor-Binding Domain Recombinant Subunit COVID-19 Vaccine Induces Strong Immune Responses in Mice. *Archives of Microbiology and Immunology*. 7 (2023): 408-420.

44. Yang S, Li Y, Dai L, Wang J, He P, Li C, et al. Safety and immunogenicity of a recombinant tandem-repeat dimeric RBD-based protein subunit vaccine (ZF2001) against COVID-19 in adults: two randomised, double-blind, placebo-controlled, phase 1 and 2 trials. *Lancet Infect Dis* 21 (2021): 1107–1119.
45. Li X, Wang L, Liu J, Fang E, Liu X, Peng Q, et al. Combining intramuscular and intranasal homologous prime-boost with a chimpanzee adenovirus-based COVID-19 vaccine elicits potent humoral and cellular immune responses in mice. *Emerg Microbes Infect* 11 (2022): 1890–1899.
46. Plotkin SA. Correlates of protection induced by vaccination. *Clin Vaccine Immunol* 17 (2010): 1055–1065.